Robust Transmural Electrophysiological Imaging: Integrating Sparse and Dynamic Physiological Models into ECG-Based Inference

Jingjia Xu[1], John L. Sapp[2], Azar Rahimi Dehaghani[1], Fei Gao[3], Milan Horacek[2], and Linwei Wang[1]

[1] Rochester Institute of Technology, Rochester, NY, 14623, USA
xujingjia.zju@gmail.com
[2] Dalhousie Unviersity,Halifax, NS, Canada
[3] Molecular Imaging Division, Siemens Medical Solutions, Knoxville, TN, 37932, USA

Abstract. Noninvasive inference of patient-specific intramural electrical activity from surface electrocardiograms (ECG) lacks a unique solution in the absence of prior assumptions. While 3D cardiac electrophysiological models emerged to be a viable vehicle for constraining this inference with knowledge about the spatiotemporal dynamics of cardiac excitation, it is important for the inference to be robust to errors in these high-dimensional model predictions given the limited ECG data. We present an innovative solution to this problem by exploiting the low-dimensional structure of the solution space – a powerful regularizer in overcoming the lack of measurements – *within* the dynamic inference guided by physiological models. We present the first Bayesian inference framework that allows the exploration of both the spatial sparsity of cardiac excitation and its complex nonlinear spatiotemporal dynamics for an improved inference of patient-specific intramural electrical activity. The benefit of this integration is verified in both synthetic and real-data experiments, where we present one of the first detailed, point-by-point comparison of the reconstructed electrical activity to *in-vivo* catheter mapping data.

1 Introduction

Despite significant advances in diagnostic imaging, a considered gap remains between the way to assess cardiac electrical and mechanical functions. To date, clinical assessment of cardiac electrophysiology remains at a gross view with several electrocardiogram (ECG) traces, while a more detailed image requires a invasive mapping using catheters. This gap has motivated the research in *noninvasive electrophysiological (EP) imaging* that, in analogy to computed tomography, collects ECG data external to the body and computationally reconstructs patient-specific electrical activity [1]. It underscores a notoriously ill-posed inverse problem: surface ECG is not only limited in number but, more importantly, different intramural electrical sources may produce identical ECG data [2].

To bypass the challenge of non-unique intramural solutions, a common approach has been to restrict the reconstruction to the surface of the heart [1].

N. Navab et al. (Eds.): MICCAI 2015, Part II, LNCS 9350, pp. 519–527, 2015.
DOI: 10.1007/978-3-319-24571-3_62

Therefore, to obtain a unique intramural solution, proper assumptions must be made. In the few existing approaches, 3D excitation models have emerged to be a useful constraint for ECG-based inference, containing rich physiological knowledge about the spatiotemporal electrical dynamics within the myocardium [3]. However, since the ECG data is limited relative to the high-dimensional model prediction, it becomes important for ECG-based inference to be robust to *priori* model errors. In dynamic inference, a common solution is to augment the unknown system state with auxiliary variables representing unknown model errors [4]. Although this allows the prior model to adapt to measurement data, it leads to an even higher-dimensional unknown space. Outside the traditional regime of dynamic inference, the low-dimensional structure of a signal (*i.e.*, its sparsity in a certain basis) has become a powerful regularizer to overcome the lack of measurements by focusing on the most important region of a high-dimensional solution space [5]. Its use in noninvasive EP imaging was recently reported [6,1], *e.g.*, by extracting the sparsity of action potential in the gradient domain using total-variation [6]. However, sparse reconstructions are mostly studied in a static context in separation from dynamic inference. In the few recent efforts toward dynamic sparse inference, a linear dynamic model is typically used to describe the slow-changing property of the sparse signal in time [7].

In this paper, we present a hierarchical Bayesian approach to integrate dynamic physiological knowledge with sparse constraint in ECG-based inference of transmural electrical activity. It allows the incorporation of: 1) complex physiological knowledge produced by quasi Monte Carlo simulation of 3D cardiac excitation models, which can be of arbitrary form and nonlinearity running as a blackbox behind the inference; and 2) sparsity structure of intramural action potential emphasizing its spatial gradient localized between active and inactive regions. These two models are mutually complementary: while the former provides inference with complex domain knowledge about nonlinear spatiotemporal dynamics, the latter addresses the inference robustness by emphasizing the low-dimensional structure in the high-dimensional model prediction. The benefit of this integration is first verified in synthetic experiments designed to test the robustness of the inference to errors in *a priori* physiological knowledge. Its capacity in complex pathological applications is then demonstrated in a pilot study on post-infarction ventricular tachycardia patients, where the reconstructed excitation maps are quantitatively verified with *in-vivo* catheter mapping data.

2 Methods

Cardiac electrical excitation produces voltage data on the body surface following the *quasi-static* electromagnetism [2]. With numerical discretization of the heart-torso anatomy of a given subject, a biophysical model $\phi_k = \mathbf{H}\mathbf{u}_k$ can be derived that relates transmural action potential $\mathbf{u}_k$ to surface ECG data ϕ_k at each time instant k. $\mathbf{H}$ is specific to each individual's anatomy and typically assumed time-invariant to simplify the inference problem. In the Bayesian setting, the likelihood $p(\phi_k|\mathbf{u}_k, \varepsilon)$ can be modeled as a normal distribution $\mathcal{N}(\mathbf{H}\mathbf{u}_k, \varepsilon\mathbf{I})$, where ε denotes the precision (inverse variance) of data error.

Prior decomposition: To exploit the sparse structure of $\mathbf{u}_k$ while utilizing physiological knowledge regarding its spatiotemporal dynamics, we introduce an extra layer into the Bayesian hierarchy to decompose $\mathbf{u}_k$ into two independent variables $\mathbf{s}_k$ and $\mathbf{t}_k$, each incorporating the corresponding signal structure of $\mathbf{u}_k$. We consider a simple decomposition model $\mathbf{u}_k = \mathbf{s}_k \cdot \mathbf{t}_k + \delta$, where $\cdot$ denotes dot product and δ is a zero-mean Gaussian residual with precision β. We obtain:

$$\mathrm{p}(\mathbf{u}_k|\mathbf{s}_k, \mathbf{t}_k, \beta) = \mathcal{N}(\mathbf{s}_k \cdot \mathbf{t}_k, \beta\mathbf{I}) \tag{1}$$

Physiological dynamic prior: $\mathbf{t}_k$ in (1) is a dimension-less descriptor of the nonlinear temporal profile of action potential. Physiological knowledge regarding its spatiotemporal behavior can be incorporated through a 3D cardiac EP model. In general, the presented framework can incorporate models as a blackbox running behind the inference. Here, the monodomain *Aliev-Panfilov* model [8] will be used to balance physiological plausibility and computational complexity:

$$\begin{cases} \frac{\partial \mathbf{t}}{\partial t} = \nabla \cdot (\mathbf{D}\nabla\mathbf{t}) + k\mathbf{t} \cdot (\mathbf{t} - a) \cdot (1 - \mathbf{t}) - \mathbf{t} \cdot \mathbf{v} \\ \frac{\partial \mathbf{v}}{\partial t} = -e(\mathbf{v} + k\mathbf{t} \cdot (\mathbf{t} - a - 1)) \end{cases} \tag{2}$$

where $\mathbf{v}$ stands for recovery current and the diffusion tensor $\mathbf{D}$ is considered anisotropic. The 3D myocardial fiber structure is mapped from an *ex-vivo* ventricular fibrous model [9]. The rest of the parameters are adopted from literature [8],so that no patient-specific pathological knowledge is assumed *a priori*.

Given posterior distribution of $\mathbf{t}_{k-1}$, the prior distribution of $\mathbf{t}_k$ can be predicted according to (2). Due to the nonlinearity of this model, a close-form prediction is not possible. Instead, simulation-based approach is used where a set of samples is drawn from the posterior distribution of $\mathbf{t}_{k-1}$ and individually passed through the excitation model; deterministic sampling based on the *unscented transform* [10] is used to reduce the number of samples needed for the high-dimensional $\mathbf{t}$ ($\sim 10^3$). The mean $\bar{\mathbf{t}}_k^-$ and covariance $\mathbf{P}_{\mathbf{t}_k}^-$ of the new samples are used to approximate the prior distribution of $\mathbf{t}_k$ as:

$$p(\mathbf{t}_k|\phi_{1:k-1}) \sim \mathcal{N}(\bar{\mathbf{t}}_k^-, \mathbf{P}_{\mathbf{t}_k}^- + \mathbf{Q}_k) \tag{3}$$

where $\mathbf{Q}_k$ is a pre-defined covariance matrix to account for errors in the prior excited model (2) caused by factors such as heart motion, fiber model, etc. Variable $\mathbf{v}$ is not modeled or inferred because it is not directly related to the measurement. Note that the sampling and model simulation runs as a blackbox behind the inference, allowing a flexible *plug-and-play* of different EP models.

Sparse prior: The error covariance $\mathbf{Q}_k$ is only able to account for errors in the prior excitation model (2) to an extent. Since the model prediction is much higher in dimension than ECG data, additional structure of the solution space should be explored to avoid the inference being dominated by model predictions. Recent studies show that the sparsity of action potential in its gradient domain (*i.e.*, localized gradient between active and inactive regions) is an effective regularizer for ECG-based inference [6]. Thus, we define a spatial profile $\mathbf{s}_k$ for action potential and approximate the continuous form of its total-variation with a numerical integration using $N_g \sim 10^5$ Gaussian quadrature points:

$$\mathrm{TV}(\mathbf{s}_k) = \int_{\Omega_h} |\nabla s_k| d\Omega_h \approx \Sigma_{i=1}^{N_g} \sqrt{\mathbf{s}_k^T \nabla \varphi_i^T \nabla \varphi_i \mathbf{s}_k} \tag{4}$$

where ∇s_k on each Gauss point is approximated by a linear combination of its neighboring nodes in the discrete ventricular mesh using shape functions φ_i.

Accordingly, the sparsity prior can be written as:

$$\mathrm{p}(\mathbf{s}_k|\alpha) = c\alpha^{2m}\exp(-\alpha \mathrm{TV}(\mathbf{s}_k)) = c\alpha^{2m}\exp[-\alpha\Sigma_{i=1}^{N_g}\sqrt{\mathbf{s}_k^T\nabla\varphi_i^T\nabla\varphi_i\mathbf{s}_k}] \quad (5)$$

where c is constant, m is the dimension of $\mathbf{s}_k$.

Hyperparameters: The precision parameters (α, β and ε) of the above distributions control their relative contributions to the inference. To reduce the reliance on an *ad-hoc* tuning of these parameters, we assume them to be unknown with Gamma distributions (the conjugate of Gaussian distributions) [11].

Hierarchical Bayesian model: Because the excitation model (2) involves a first-order derivative in time, it is reasonable to assume $\mathbf{t}_k$ to be a first-order Markov process. The prior for sparsity and all hyperparameters can be assumed to be not informed by the previous ECG data, *i.e.*, independent with $\phi_{1:k-1}$:

$$\mathrm{p}(\mathbf{s}_k|\alpha,\phi_{1:k-1}) \equiv \mathrm{p}(\mathbf{s}_k|\alpha), \quad \mathrm{p}(\theta|\phi_{1:k-1}) \equiv \mathrm{p}(\theta), \theta \in \{\alpha,\beta,\varepsilon\} \quad (6)$$

Therefore, given ECG data $\phi_{1:N}$ throughout N time instants in a cardiac cycle, we can recursively compute the joint posterior distribution of all the unknowns $\Theta_k = (\mathbf{u}_k, \mathbf{t}_k, \mathbf{s}_k, \alpha, \beta, \varepsilon)$ given the data available up to the time instant k:

$$\begin{aligned}&\mathrm{p}(\Theta_k|\phi_{1:k}) \propto \mathrm{p}(\phi_k|\Theta_k)\mathrm{p}(\Theta_k|\phi_{1:k-1})\\ &= \mathrm{p}(\phi_k|\mathbf{u}_k,\varepsilon)\mathrm{p}(\mathbf{u}_k|\mathbf{t}_k,\mathbf{s}_k,\beta)\mathrm{p}(\mathbf{t}_k|\phi_{1:k-1})\mathrm{p}(\mathbf{s}_k|\alpha)\mathrm{p}(\alpha)\mathrm{p}(\beta)\mathrm{p}(\varepsilon)\end{aligned} \quad (7)$$

Fig. 1(a) outlines the hierarchical Bayesian model at one time instant.

Variational Bayesian inference: The posterior distribution in (7) is analytically intractable. We adopt the variational Bayesian method to seek a tractable distribution $\mathrm{q}(\Theta_k)$ with minimal Kullback-Leibler (KL) divergence to (7):

$$\hat{q}(\Theta_k) = \arg\min_{q(\Theta_k)} C_{KL}(\mathrm{q}(\Theta_k)\|\mathrm{p}(\Theta_k|\Phi_{1:k})) = \int \mathrm{q}(\Theta_k)\log(\frac{\mathrm{q}(\Theta_k)}{\mathrm{p}(\Theta_k|\Phi_{1:k})})d\Theta \quad (8)$$

The solution to the above optimization problem is given by:

$$\mathrm{q}(\Theta_{k,i}) \propto \exp(\mathrm{E}_{\Theta\setminus\Theta_{k,i}}[\ln \mathrm{p}(\Theta_k,\Phi_{1:k})]) \quad (9)$$

where $\mathrm{E}_{\Theta_k\setminus\Theta_{k,i}}[\cdot]$ denotes the expectation with respect to all variables in the set of Θ_k except the variable of interest $\Theta_{k,i}$. Because the total-variation prior (5) prevents us from solving equation (9) analytically, we introduce an auxiliary vector $\mathbf{w}$ and define $\mathrm{p}(\mathbf{s}_k,\mathbf{w}|\alpha) = c\alpha^{\gamma m}\exp(-\frac{\alpha}{2}\sum_i^{N_g}\frac{\mathbf{s}_k^T\nabla\varphi_i^T\nabla\varphi_i\mathbf{s}_k+w_i}{\sqrt{w_i}})$. Because $\mathrm{p}(\mathbf{s}_k,\mathbf{w}|\alpha) \leq \mathrm{p}(\mathbf{s}_k|\alpha)$ given the geometric-arithmetic mean inequality, replacing $\mathrm{p}(\mathbf{s}_k|\alpha)$ with $\mathrm{p}(\mathbf{s}_k,\mathbf{w}|\alpha)$ in equation (8) gives us an upper bound of the KL divergence. We can thus recursively minimize and monotonically decrease this upper bound until convergence to the original solution to (8) [11]. We randomly initialize $\mathbf{u}^1$ and then enter an iterative procedure. In each iteration, we cycle through each variable in Θ_k to update its posterior distribution according to (9). The main algorithm flow is illustrated in Fig. 1(b).

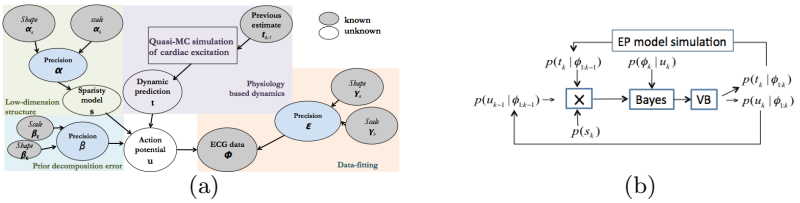

(a) (b)

Fig. 1. Illustration of the hierarchical Bayesian model (a) and algorithm flow (b).

3 Experiments and Results

3.1 Simulation Study

Synthetic experiments are designed on pathological conditions to test the robustness of the inference to errors in *a priori* models. Experiments are conducted on 3 realistic human heart-torso models derived from CT scans (heart: $\sim$ 2000 meshfree nodes; torso: 120 nodes). In all experiments, simulated time sequences of 120-lead ECGs are corrupted with 20-db white Gaussian noise. We compare the presented method with that constrained by 1) dynamic excitation model only [3] and 2) sparse total-variation model only [6]. The accuracy is measured by *correlation coefficient* (CC) between the reconstructed and simulated sequences of action potential.

Myocardial infarction: 10 cases of myocardial infarction are test, where ventricular action potential is simulated with the model(2) using parameters modified at the region of infarct scar [8]. It is noteworthy that the inference is guided by models with standard parameters, invoking *a priori* model parameter errors.

Fig. 2(a) top row shows snapshots of the simulated propagation of action potential during apical pacing with an infarct localized at the mid-basal lateral region of the LV (labeled by purple line). Before the excitation encounters (a1) or after it leaves the infarct region (a4), the *a priori* model error is minimal; therefore, result constrained by the excitation model shows high consistence with the ground truth (row 2 & 3). However, as the wavefront encounters and gets disrupted by the infarct region (a2), prior model errors start to have a visible impact on the solution accuracy (a2; row 3). In comparison, our method accurately reconstructs the abnormal excitation caused by the anatomical block, *demonstrating an improved robustness to model errors brought by simultaneously focusing on the sparse structure of the solution* (a2; row 2). During ECG ST-segment (a3), constrained by the dynamic model only, the inference is only able to overcome the model error and to reflect the inactive necrosis to a certain extent (a3; row 2); the exploit of sparse structure evidently improve this ability (a3; row 3): two additional examples from ECG ST-segments on different infarcted hearts are listed in Fig. 2(b). Inspection of the reconstructed temporal waveform of action potential tells a similar story (Fig. 2(2-3)): when strong prior dynamic knowledge is imposed, exploiting the low-dimensional structure of intramural action potential helps the inference to better combat the error in this knowledge.

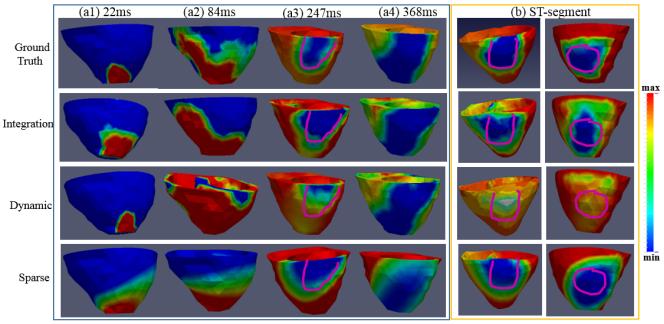

Fig. 2. Snapshots of intramural action potential propagation on infarcted hearts: simulated ground truth *vs.* inferences with physiological dynamic constraint only (Dynamic), sparsity constraint only (Sparse), and combined constraints (Integration).

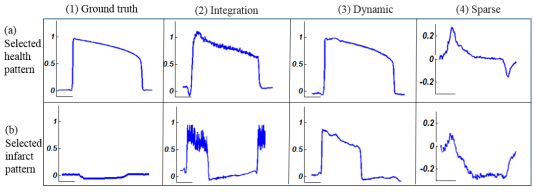

Fig. 3. Temporal morphology of simulated and reconstructed action potential.

Conversely, when only sparsity model is used, the inference is successful in capturing a gross division between active versus inactive regions. However, the excitation wavefront loses its intricate details (Fig. 2(a4)) and, more importantly, temporal morphology of action potential cannot be reproduced (Fig. 2(4)).

Premature ventricular contraction (PVC): In another 5 set of experiments, we consider abnormal ectopic foci that are not known *a priori* in the sinus-rhythm excitation model. Thus, the relevant model error primarily occurs in the early stage of ventricular excitation. As shown in Fig. 3.1(a), inference constrained by the dynamic model shows erroneous activation at standard sinus-rhythm sites. The integration with sparsity models is able to help correct this model error and produce PVC sites close to the simulated ground truth.

Statistical analysis: Quantitative analysis on CC are summarized in all cases across both settings. Fig. 3.1(b1) shows CC calculated on the complete temporal sequence of reconstructed action potential: in comparison to using sparsity models only, the use of prior excitation models can significantly improve CC by providing temporal morphology that is physiologically correct ($p < 0.01$, paired-t). Fig. 3.1(b2) shows CC calculated on the first half sequence within the cardiac cycle when less ECG data are available to the inference: in comparison to using dynamic models only, the exploitation of sparsity significantly improves CC by better overcoming model errors given limited data ($p < 0.01$, paired-t).

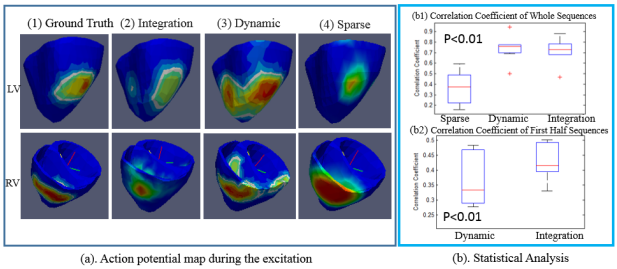

Fig. 4. Snapshots of intramural action potential resulting from ectopic foci (a) and correlation coefficients across n=15 synthetic cases (b).

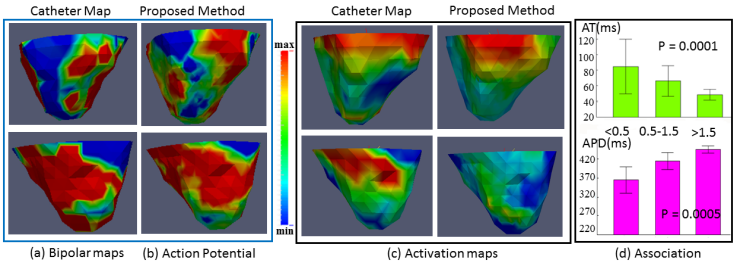

Fig. 5. Comparison with invasive catheter mapping on a post-infarction patient.

3.2 Real-Data Study

A case study is conducted on a patient who underwent catheter ablation of scar-related ventricular tachycardia. Transmural action potential is inferred from 120-lead ECG data on CT-derived anatomical model. *In-vivo* bipolar voltage map (Fig. 5(a1)) was collected during invasive EP study, where two low-voltage regions were revealed at lateral RV and lateral-basal LV (dense scar: blue, $\leq$ 0.5mV; scar border: green, 0.5-1.5mV). Action potential reconstructed by our method during ECG ST-segment exhibits low amplitude at the same regions (Fig. 5(a2)). Fig. 5(b1) shows the invasive activation map acquired on the same patient in stable rhythm: comparing activation (b1) and voltage maps (a1) side by side, we can appreciate the intrinsic native-rhythm activation within the low-voltage region. This is consistent with recent study that some critical isthmuses may exist within low-voltage areas, underscoring the importance of an accurate, high-resolution activation map in identifying culprit tissue for surgery planning [12]. Fig. 5(b2) illustrates the activation map obtained from our method, which exhibits similar pattern to the invasive map and is able to delineate intrinsic electrical activity around low-voltage regions.

Statistical analysis on 208 epicardial points (Fig. 5(c)) verified a negative association between the reconstructed activation time and bipolar voltage ($p = 0.0002$, Spearman's ρ), and a positive association between the reconstructed action potential duration and bipolar voltage ($p = 0.0001$, Spearman's ρ). With decreasing voltage, significant differences are also found in three action potential

features: delay of activation ($p = 0.001$, ANOVA), reduction of duration ($p = 0.005$, ANOVA), and increase of repolarization heterogeneity ($p < 0.05$, F-test for standard deviation). These changes are consistent with documented action potential biomarkers associated with ischemic hearts [12].

3.3 Conclusion

This paper has two major contributions: 1) the improved robustness of transmural EP imaging will contribute to its reliable clinical use; this is also one of the first studies to associate noninvasive solutions with *in-vivo* catheter maps on human subjects; and 2) bridging the gap between dynamic inference and sparse regularization, this is to our knowledge the first theoretical framework for statistical inference that supports the use of the low-dimensional structure in concurrence with its domain knowledge yielded by complex nonlinear dynamic models. It provides a novel solution to the general challenge regarding the robustness of dynamic inference to *a priori* model errors. Future work will study the robustness of this framework to additional model errors, *i.e.* cardiac motion, cardiac fiber model and the setting of algorithm parameters. Note that, due to the difficulty of invasive mapping, its discrepancy with noninvasive solutions should be interpreted with caution.

Acknowledgement. This work is supported by the National Science Foundation under CAREER Award ACI-1350374 and the National Institute of Heart, Lung, and Blood of the National Institutes of Health under Award R21Hl125998.

References

1. Ghosh, S., Rudy, Y.: Application of l1-norm regularization to epicardial potential solutions of the inverse electrocardiography problem. Annals of Biomedical Engineering 37, 902–912 (2009)
2. Plonsey, R.: Bioelectric phenomena. Wiley Online Library (1999)
3. Wang, L., Dawoud, F., Yeung, S.K., Shi, P., Wong, K.C., Liu, H., Lardo, A.C.: Transmural imaging of ventricular action potentials and post-infarction scars in swine hearts. IEEE Transactions on Medical Imaging 32, 731–747 (2013)
4. Haykin, S.: Adaptive Filter Theory. Prentice Hall (1996)
5. Candes, E.J., Romberg, J., Tao, T.: Robust uncertainty principles: Exact signal reconstructions from highly incomplete frequency information. IEEE Transactions on Information Theory 52, 489–509 (2006)
6. Xu, J., Dehaghani, A., Gao, F., Wang, L.: Noninvasive transmural electrophysiological imaging based on minimization of total-variation functional. IEEE Transactions on Medical Imaging 33, 1860–1874 (2014)
7. Carmi, A., Gurfil, P., Kanevsky, D.: Methods for sparse signal recovery using kalman filtering with embedded pseudo-measurement norms and qausi-norms. IEEE Transactions on Signal Processing 58, 2405–2409 (2010)
8. Aliev, R.R., Panfilov, A.V.: A simple two-variable model of cardiac excitation. Chaos, Solitons & Fractals 7, 293–301 (1996)

9. Nash, M.: Mechanics and Material Properties of the Heart using an Anatomically Accurate Mathematical Model. PhD thesis, Univ. of Auckland (1998)
10. Julier, S.: The scaled unscented transform. International Journal for Numerical Methods in Engineering 47, 1445–1462 (2000)
11. Smídl, V., Quinn, A.: The variational Bayes method in signal processing. Springer (2006)
12. Jamil-Copley, S., Vergara, P., Carbucicchio, C., et al.: Application of ripple mapping to visualise slow conduction channels within the infarct-related left ventricular scar. Circulation Arrhythmia and Electrophysiology (2014). Epub ahead of print